# TDP-43-associated atrophy in brains with and without frontotemporal lobar degeneration

Marina Buciuc [a], Peter R. Martin [b], Nirubol Tosakulwong [b], Melissa E. Murray [c], Leonard Petrucelli [c], Matthew L. Senjem [d], Anthony J. Spychalla [d], David S. Knopman [a], Bradley F. Boeve [a], Ronald C. Petersen [a], Joseph E. Parisi [e], R. Ross Reichard [e], Dennis W. Dickson [c], Clifford R. Jack Jr. [d], Jennifer L. Whitwell [d], Keith A. Josephs [a],*

[a] *Department of Neurology, Mayo Clinic, 200 1st Street NW, Rochester, MN 55905, USA*
[b] *Department of Quantitative Health Sciences, Mayo Clinic, 200 1st Street NW, Rochester, MN 55905, USA*
[c] *Department of Neuroscience, Mayo Clinic, 4500 San Pablo Rd S, Jacksonville, FL 32224, USA*
[d] *Department of Radiology, Mayo Clinic, 200 1st Street NW, Rochester, MN 55905, USA*
[e] *Department of Laboratory Medicine and Pathology, Mayo Clinic, 200 1st Street NW, Rochester, MN 55905, USA*

## ARTICLE INFO

## ABSTRACT

Transactive response DNA-binding protein of ~43 kDa (TDP-43), a primary pathologic substrate in tau-negative frontotemporal lobar degeneration (FTLD), is also often found in the brains of elderly individuals without FTLD and is a key player in the process of neurodegeneration in brains with and without FTLD. It is unknown how rates and trajectories of TDP-43-associated brain atrophy compare between these two groups. Additionally, non-FTLD TDP-43 inclusions are not homogeneous and can be divided into two morphologic types: type-α and neurofibrillary tangle-associated type-β. Therefore, we explored whether neurodegeneration also varies due to the morphologic type. In this longitudinal retrospective study of 293 patients with 843 MRI scans spanning over ~10 years, we used a Bayesian hierarchical linear model to quantify similarities and differences between the non-FTLD TDP-43 (type-α/type-β) and FTLD-TDP (n = 68) in both regional volume at various timepoints before death and annualized rate of atrophy. Since Alzheimer's disease (AD) is a frequent co-pathology in non-FTLD TDP-43, we further divided types α/β based on presence/absence of intermediate-high likelihood AD: AD-TDP type-β (n = 90), AD-TDP type-α (n = 104), and Pure-TDP (n = 31, all type-α). FTLD-TDP was associated with faster atrophy rates in the inferior temporal lobe and temporal pole compared to all non-FTLD TDP-43 groups. The atrophy rate in the frontal lobe was modulated by age with younger FTLD-TDP having the fastest rates. Older FTLD-TDP showed a limbic predominant pattern of neurodegeneration. AD-TDP type-α showed faster rates of hippocampal atrophy and smaller volumes of amygdala, temporal pole, and inferior temporal lobe compared to AD-TDP type-β. Pure-TDP was associated with slowest rates and less atrophy in all brain regions. The results suggest that there are differences and similarities in longitudinal brain volume loss between FTLD-TDP and non-FTLD TDP-43. Within FTLD-TDP age plays a role in which brain regions are the most affected. Additionally, brain atrophy regional rates also vary by non-FTLD TDP-43 type.

## 1. Introduction

Transactive response DNA-binding protein of ~43 kDa (TDP-43) gained international attention after its discovery as the primary pathologic substrate in tau-negative frontotemporal lobar degeneration (FTLD) and amyotrophic lateral sclerosis (Arai et al., 2006; Neumann et al., 2006) which opened a new avenue for research. In addition to unraveling the role of TDP-43 in FTLD, its implication in pathophysiology and clinical presentation of other neurodegenerative diseases has been widely studied (Arai et al., 2009; Buciuc et al., 2020b; Hasegawa et al., 2007; Higashi et al., 2007; James et al., 2016; Josephs et al., 2019a; Josephs et al., 2008; Josephs et al., 2014b; Nag et al., 2017; Nelson et al., 2019; Nelson et al., 2011).

Pathologically, patients with "typical" young onset FTLD-TDP have focal gross atrophy in frontal and/or temporal lobes and microvacuolation in these regions (Cairns et al., 2007), as well as abnormal TDP-43 deposition (Mackenzie et al., 2006; Mackenzie et al., 2011; Mackenzie et al., 2009). However, TDP-43 pathology is also often found in the brains of elderly individuals without FTLD. In these non-FTLD cases, TDP-43 often co-exists with Alzheimer's disease (AD-TDP) but can occur in relative isolation (pure-TDP) (Amador-Ortiz et al., 2007; Buciuc et al., 2020b; Josephs et al., 2014b; Nelson et al., 2019; Nelson et al., 2011; Robinson et al., 2018). In our earlier work we demonstrated that TDP-43 in non-FTLD cases is independently associated with faster rates of hippocampal atrophy and also faster cognitive decline, thus, earning its place as one of the key players of neurodegeneration rather than a co-pathology of uncertain consequences (Buciuc et al., 2021a; Buciuc et al., 2020a; Josephs et al., 2017). We then further demonstrated that the hippocampus is the most vulnerable region to TDP-43 in non-FTLD cases, although TDP-43 has also been found to be associated with faster rates of brain atrophy in the inferior temporal and frontal lobes (Bejanin et al., 2019; Josephs et al., 2020). Importantly, TDP-43-associated rates of brain atrophy are non-linear over the course of the disease (Josephs et al., 2020). There is still, however, a void in our understanding of how neurodegeneration in FTLD-TDP compares to AD-TDP and pure-TDP, longitudinally.

While FTLD-TDP is subclassified into five types based on morphology and distribution of TDP-43 immunoreactive inclusions which also correlates with specific clinical phenotypes (Mackenzie et al., 2011), in non-FTLD brains TDP-43 inclusions can also be subtyped into two types (Josephs et al., 2019b) including TDP-43 type-α resembling FTLD-TDP type A (Mackenzie et al., 2011), and neurofibrillary tangle (NFT) associated TDP-43 type-β. The distinction of these types is supported by differences in age, genetics, co-pathologies, molecular patterns, patterns of brain atrophy, and clinical implications (Buciuc et al., 2020c; Josephs et al., 2019b; Tomé et al., 2020). It is also unknown how anatomic patterns and rates of atrophy differ between types in non-FTLD types.

To address these above-mentioned gaps in knowledge, we perform an MRI-histological-Bayesian analysis whereby we investigate how rate and degree of regional brain atrophy differs between FTLD-TDP, AD-TDP and pure-TDP, and how rates differ between AD-TDP types-α and β. We hypothesize that AD-TDP types will be associated with higher rates of atrophy in the hippocampus, whereas FTLD-TDP cases would have the highest rates of atrophy in the frontal lobe.

## 2. Materials and methods

### 2.1. Patients and healthy controls

We identified all patients who had been recruited and prospectively followed in the National Institute of Health-funded Mayo Clinic Alzheimer's Disease Research Center or Mayo Clinic Study of Aging, had died with brain autopsy between 1 January 1992 and 31 December 2015, had TDP-43 positive inclusions in at least one brain region and at least one useable antemortem volumetric head MRI. Age at death, sex and closest to death clinical diagnosis were abstracted from the medical records. This study has been approved by the Mayo Clinic institutional review board, and all patients and/or their proxies signed a written informed consent form before taking part in any research activities in accordance with the Declaration of Helsinki.

### 2.2. Pathologic evaluation

#### 2.2.1. TDP-43 group assignment

Cases were rendered as TDP-43-positive if any TDP-43 immunoreactive inclusions were identified with anti-TDP-43 polyclonal antibody (MC2085, from Professor Leonard Petrucelli) (Zhang et al., 2009) that recognizes a peptide sequence in the 25-kDa C-terminal fragment on a DakoAutostainer (Dako-Cytomaton) and 3,30-diaminobenzidine as the chromogen. FTLD-TDP was diagnosed pathologically in cases with focal macroscopic degeneration of the frontal and/or temporal lobes and/or microscopic evidence of microvacuolation, neuronal loss and astrogliosis particularly in laminar II or transcortical layers (Cairns et al., 2007; Mackenzie et al., 2009). FTLD-TDP types A – C (Mackenzie et al., 2011) were included in this group. We did not have any type D or E cases. All FTLD-TDP cases were screened for mutations in progranulin (Baker et al., 2006) and *C9ORF72* (DeJesus-Hernandez et al., 2011; Renton et al., 2011), as previously described (Whitwell et al., 2012b). All other TDP-43 positive cases not meeting criteria for FTLD diagnosis were categorized as either AD-TDP or pure-TDP depending on the presence and amount of AD pathology; AD-TDP cases were classified as those with intermediate/high likelihood of ADNC, and pure-TDP cases were classified as those with none/low likelihood of AD neuropathologic changes (ADNC) (Buciuc et al., 2021b; Hyman et al., 2012; Montine et al., 2012). For all AD-TDP and pure-TDP cases the amygdala, subiculum, CA1 and dentate gyrus of the hippocampus, entorhinal, occipitotemporal, inferior temporal, basal forebrain, insular, ventral striatum and middle frontal cortices, as well as basal ganglia and brainstem regions were screened for TDP-43 immunoreactive inclusions to assign one of the six Josephs TDP-43 stages (Josephs et al., 2014a; Josephs et al., 2016). A case was determined to be TDP-43 type-α when TDP-43-immunoreactive neuronal cytoplasmic inclusions, dystrophic neurites, and/or neuronal intranuclear inclusions were the only or predominantly detected lesions, or TDP-43 type-β when TDP-43-immunoreactivity adjacent to tau-immunoreactive NFTs was the predominant feature of the observed TDP-43 lesions in one or more regions (Josephs et al., 2019b).

#### 2.2.2. ADNC and other pathologies

All cases were evaluated according to standard neuropathologic examination following cortical sampling according to the Consortium to Establish a Registry for Alzheimer's disease (CERAD) (Mirra et al., 1991) with thioflavin S fluorescent microscopy used to assign Braak NFT stage (Braak et al., 2006), and CERAD neuritic plaque score. Braak NFT stages were collapsed to B1 (Braak stages I + II), B2 (Braak stages III – IV), and B3 (Braak stages V – VI). Scoring of neuritic plaques in neocortex was the following: C0 = none; C1 = sparse neuritic plaques; C2 = moderate neuritic plaques; C3 = frequent neuritic plaques. All cases were assigned ADNC likelihood based on the National Institute of Aging-Reagan (Hyman and Trojanowski, 1997) and National Institute of Aging -Alzheimer's Association criteria (Hyman et al., 2012).

The presence of vascular lesions (micro-infarcts, lacunar infarcts [<1cm], large infarcts [≥ 1 cm]) was recorded. A four-point vascular score (0 – 3) was used to grade cerebrovascular disease: 0 = no vascular lesions; 1 = only micro-infarcts present; 2 = presence of lacunar or large infarcts but no micro-infarcts; 3 = presence of micro-infarcts and lacunar or large infarcts.

The presence of Lewy bodies in amygdala, limbic, brainstem or neocortical regions was documented in accordance with published consensus report (McKeith et al., 2017) with 0 = no Lewy bodies, 1 = brainstem-predominant Lewy body disease (LBD), 2 = amygdala-predominant or limbic/transitional LBD, 3 = diffuse/neocortical LBD.

## 2.3. MRI analyses

All MR scans were performed using a standardized protocol that included a T1-weighted 3D volumetric sequence (Jack et al., 2008). Over the period of 23 years, the cohort was scanned on a mixture of 1.5 T (690 scans, 82%) and 3 T (153 scans, 18%) General Electric (GE) scanners. At 1.5 T, spoiled gradient recalled echo sequences were acquired (124 contiguous partitions, 1.6 mm slice thickness, 24 × 18.5 cm field of view, minimum full TE, TR 23 ms, and 25° flip angle) and at 3 T, magnetization prepared rapid gradient echo sequences were acquired (TR/TE/T1, 2300/3/900 msec; flip angle 8°, 26 cm field of view; 256 × 256 in-plane matrix with a phase field of view of 0.94, and 1.2 mm slice thickness) (Josephs et al., 2020). Longitudinal analyses were always run using sets of serial scans performed at the same field strength. That is, subjects with 1.5 and 3.0 T scans were considered to have two independent series. All scanners undergo a standardized quality control calibration procedure daily, which monitors geometric fidelity over a 200 mm volume along all three cardinal axes, signal-to-noise, and transmit gain, and maintains the scanner within a tight calibration range.

Serial volumes were calculated using FreeSurfer version 5.3.0 (http://surfer.nmr.mgh.harvard.edu/) (Fischl et al., 2002). All scans were first run through the FreeSurfer cross-sectional pipeline and registered to a spherical atlas to match cortical geometry across the patients. A separate longitudinal FreeSurfer pipeline was run using the unbiased template and 9 degrees of freedom registration to account for scaling fluctuations. Manual inspection of segmentations was performed for all cases, and 12 patients (16 scans) were excluded due to segmentation failure. Our analysis focused on assessing regional volumes of the amygdala, hippocampus, temporal pole, inferior temporal, and middle frontal gyri. These regions were selected because these regions are affected in AD-TDP and FTLD-TDP (Cairns et al., 2007; Josephs et al., 2020).

## 2.4. Statistical analyses

The primary purpose of our analysis was to describe and differentiate regional volume and atrophy proximal to death across our TDP-43 groups. To answer many questions simultaneously, we fit a single Bayesian hierarchical linear model that encompassed all scans from all individuals. Bayesian hierarchical models are well suited to address multiple questions simultaneously by incorporating multiple collinear measurements (here, multiple regions within scan and multiple scans within individual) and using partial pooling to borrow statistical strength across regions while fairly managing the correlation structure in the data (Gelman and Hill, 2006). The resulting estimates are shrunken, both from the method of estimation in the Bayesian paradigm as well as via partial pooling, resulting in more robust and reproducible effect estimates (Greenland, 2000).

This single Bayesian hierarchical linear model spanned five brain regions using standardized volume as the outcome and both cross sectional (centered at −5 years from death) and longitudinal (years from death) region-specific effects for TDP-43 group as predictors. The standardized volume was calculated by fitting an ordinary least squares regression within each region predicted by an intercept, total intracranial volume (TIV), sex, and age at scan in a cohort of cognitively normal controls. We then used those model fits to predict expected volumes in our TDP-43 cohort, calculated the residuals, then divided these residuals by the standard deviation of the residuals from the original control-only model fits, yielding comparable measures across regions (standard deviations of healthy young volumes). Cognitively normal controls came from population-based Mayo Clinic Study of Aging and represented 216 amyloid-beta and tau negative individuals aged between 50 and 90 years old at the time of volumetric brain MRI (Roberts et al., 2008). Regional W-scored brain volumes of these individuals were used as reference for analysis.

We included additional region-specific cross-sectional effects for sex, age at death, an additional FTLD shift in age at death (to allow FTLD and AD-TDP/pure-TDP to differ in their relationship between age at death and cross-sectional volume), vascular score, LBD stage and scanner field strength. Similarly, we included region-specific longitudinal effects for vascular stage, LBD stage, age at death, an additional FTLD shift in age at death. The last model terms included were needed to fairly combine regions and scans from each individual in a single model; person-and-region specific shifts in volume and person-specific shifts in annual atrophy rates.

We can represent this model algebraically as

$$y_{rij} = \beta_{1rk} + (\beta_{2r} + \beta_{3r}*FTLD_i)*age\ at\ death_i +$$

$$\beta_{4r}*male_i + \beta_{5r}*vascular_i + \beta_{5r}*LBDstage_i + \beta_{6r}*FieldStrength_{ij} +$$

$$years\ from\ death_{ij}*(\beta_{7rk} + (\beta_{8r} + \beta_{9r}*FTLD_i)*age\ at\ death_i +$$

$$\beta_{10r}*vascular_i + \beta_{11r}*LBDstage_i) +$$

$$\gamma_{1ri} + \gamma_{2i}*years\ from\ death$$

where $r \in 1:5$ indicates region, $i \in 1:293$ indicates individual, $j \in 1:9$ indicates scan (within individual), $k \in 1:4$ indicates TDP group of an individual, $FTLD_i \in 0,1$ indicates whether individual $i$ was FTLD, $male_i \in 0,1$ indicates whether an individual $i$ was male, $vascular_i \in 0:3$ indicates the vascular stage of individual $i$, $LBDstage_i \in 0:3$ indicates the LBD stage of individual $i$, $ageatdeath_i$ is the age at death of individual $i$, $yearsfromdeath_{ij}$ indicates the years from death of individual $i$ at scan $j$, $\gamma_{1ri}$ is the person-and-region specific shift from the average regional volume and are allowed nonzero covariance across regions within person, and $\gamma_{2i}$ is the person-specific shift from the average annual atrophy rate for individuals with more than one scan and this term is assumed to be independent of the person-and-region specific terms in the model. Age at death was centered at 85 years and scaled so that one unit was equivalent to a 5-year difference in age at death. Years from death was centered at −5 to improve estimation of the cross-sectional effects. $FieldStrength_i$ represents the MRI field strength at each individual $i$ at scan $j$. More detailed information about model specification, prior distributions, and covariance structures can be found in the Statistical supplement.

The model fit used Markov Chain Monte Carlo simulation to obtain posterior distributions of each parameter. Four parallel chains of length 10,000 were used, with the first half of each thrown out as burn in, resulting in a posterior sample of 20,000 total accepted draws for each parameter. Model diagnostics showed no lack of fit. The Monte Carlo standard error was approximately zero for all parameters, the effective sample size of all parameters was in the thousands or tens of thousands, and the $\widehat{R}$ of each parameter, where values greater than one indicate lack of convergence, was approximately 1 in all cases (maximum value 1.006). In the Bayesian paradigm, we treat posterior probabilities >0.90 as evidence of a difference and consider posterior probabilities >0.99 strong evidence of a difference.

The software used to fit this model was R(Team, 2019) version 3.6.2 using the rstanarm package (Goodrich et al., 2020; Brilleman et al., 2019) version 2.21.1 running STAN version 2.21.0.

## 2.5. Data availability

Anonymized data supporting the findings of this study are available from the corresponding author upon reasonable request.

## 3. Results

A total of 293 patients with 843 usable volumetric head MRI scans were included in this study. Of these 293 patients, 170 (58%) were

female. Sixty-eight (23%) patients had a pathologic diagnosis of FTLD-TDP, of which 50 were type A, 14 type B and four type C. Thirty of the FTLD-TDP patients had an FTLD genetic mutation (15 progranulin, 15 *C9ORF72*). The median age at death for the patients with progranulin mutations was 70 years (IQR 65–80) and the median age at death for the *C9ORF72* mutation cases was 62 years (IQR 54–71). One-hundred and ninety-four patients (66%) had AD-TDP, and 31 (11%) had pure-TDP. Of those with AD-TDP 104 (54%) were type-α and 90 (46%) type-β. All type-β cases had co-existing intermediate-to-high likelihood of ADNC as expected given its association with NFTs (Josephs et al., 2019b). Therefore, we compared the degree and rates of atrophy in five brain regions in the following four pathologic groups: FTLD-TDP, AD-TDP type β, AD-TDP type α, and pure-TDP type α. Demographic, clinical, and pathologic features of these four groups are summarized in Table 1. Plotting the fits over data by region and TDP-43 group (Supplementary Fig. 1) confirmed that the chosen Bayesian hierarchical linear statistical model is appropriate for the analysis and the data fits within the designated comparison groups. In the results of the Bayesian hierarchical model we represent FTLD-TDP group as two separate age categories: a young onset with estimate centered at 65 years old at death (65yo FTLD-TDP) which is representative of our cohort and an old onset group using the FTLD-TDP age effect terms from the model to create an estimate centered at 85 years old at death (85yo FTLD-TDP) which is less representative of our FTLD-TDP cohort but allows for a more fair comparison, age-wise, to AD-TDP and pure-TDP groups.

### 3.1. Annualized rates of atrophy

Fig. 1 shows how annualized rates of atrophy of the regional volumes differ across TDP groups. We also accounted for vascular and LBD pathology, age at death, field strength and given that FTLD patients usually die younger, we introduced an additional age at death-FTLD term to account for this difference. The influence of these covariates on the imaging outcomes can be observed in Supplementary Fig. 2.

The FTLD-TDP (young and old) and AD-TDP (type α and β) groups showed similar rates of amygdala atrophy, with almost zero amygdala atrophy observed in pure-TDP (Table 2). FTLD-TDP (young and old) and AD-TDP type α were associated with the greatest rates of atrophy in the hippocampus, followed by AD-TDP type β, and then pure-TDP (Table 2). FTLD-TDP (young and old) had greater rates of atrophy in the inferior temporal lobe and temporal pole compared to AD-TDP (type-α and type-β) and Pure TDP. Similar rates of inferior temporal and temporal pole atrophy were observed in AD-TDP type α and β. Pure-TDP had the slowest rate of atrophy in all temporal regions (Table 2).

The middle frontal gyrus is the only region where rates of atrophy differed between young and old FTLD-TDP with young FTLD-TDP having the fastest rate of atrophy compared to all TDP groups. There was some evidence that old FTLD-TDP and AD-TDP type β atrophy were faster than pure-TDP and AD-TDP type α in the middle frontal gyrus (Table 2).

### 3.2. Rate of atrophy and brain volume on a time continuum

Fig. 2 summarizes the relationship between rates of atrophy and regional volumes on a continuum starting at 10 years prior to death for all four TDP groups and how they compare to controls. Table 3 complements Fig. 2 by allowing for interpretation of differences in regional brain volumes between TDP groups at two time points: 10 years prior to death and at death.

#### 3.2.1. Amygdala

AD-TDP type-β started off with larger volumes of the amygdala 10 years before death compared to AD-TDP type-α and both FTLD-TDP groups, although all four of these groups showed similar rates of atrophy. Pure-TDP did not show atrophy of the amygdala and had the largest amygdala volumes at death compared to all other groups.

**Table 1**

Demographic, clinical and pathologic characteristics by TDP-43 pathologic group.

| | FTLD-TDP Types A-C n = 68 | AD-TDP Type β n = 90 | AD-TDP Type α n = 104 | Pure-TDP Type α n = 31 | *p*-value |
|---|---|---|---|---|---|
| Female sex | 31 (46%) | 57 (63%) | 64 (62%) | 18 (58%) | 0.0931 |
| Age at death, years | 68.3 (12.2) | 84.5 (8.6) | 88.2 (6.8) | 88.7 (5.1) | 0.0001 |
| Last scan to death, years | 3.1 (2.4) | 4.0 (2.7) | 5.4 (3.0) | 3.5 (2.8) | 0.0001 |
| No. scans/patient[a] | 2 (1, 3) | 2 (1, 4) | 3 (2, 5) | 2 (2, 4) | 0.0229 |
| **Clinical diagnosis** | | | | | <0.0001 |
| Frontotemporal dementia | 45 (66%) | 3 (3%) | 0 (0%) | 0 (0%) | |
| Nonfluent primary progressive aphasia | 4 (6%) | 1 (1%) | 1 (1%) | 0 (0%) | |
| Fluent/semantic primary progressive aphasia | 9 (13%) | 0 (0%) | 0 (0%) | 0 (0%) | |
| Corticobasal degeneration syndrome | 1 (1%) | 2 (2%) | 0 (0%) | 0 (0%) | |
| Alzheimer's dementia (AD) | 7 (10%) | 63 (70%) | 81 (78%) | 7 (26%) | |
| Amnestic mild cognitive impairment (MCI) | 0 (0%) | 4 (4%) | 5 (5%) | 4 (13%) | |
| Non-amnestic MCI | 0 (0%) | 1 (1%) | 0 (0%) | 0 (0%) | |
| Multiple domain MCI without amnestic component | 1 (1%) | 0 (0%) | 0 (0%) | 0 (0%) | |
| Multiple domain MCI with amnestic component | 0 (0%) | 2 (2%) | 2 (2%) | 0 (0%) | |
| Dementia with Lewy bodies | 0 (0%) | 3 (3%) | 7 (7%) | 1 (1%) | |
| Dementia-unclassifiable | 1 (1%) | 2 (2%) | 1 (1%) | 0 (0%) | |
| Multi-infarct | 0 (0%) | 3 (3%) | 2 (2%) | 0 (0%) | |
| Brain tumor | 0 (0%) | 1 (1%) | 0 (0%) | 0 (0%) | |
| No impairment | 0 (0%) | 6 (7%) | 4 (4%) | 18 (58%) | |
| **Pathologic characteristics** | | | | | |
| TDP-43 stage | | | | | <0.0001 |
| 1 | 0 (0%) | 29 (32%) | 3 (3%) | 8 (26%) | |
| 2 | 0 (0%) | 36 (40%) | 8 (8%) | 1 (3%) | |
| 3 | 0 (0%) | 10 (11%) | 15 (14%) | 3 (10%) | |
| 4 | 0 (0%) | 11 (12%) | 35 (34%) | 5 (16%) | |
| 5 | 0 (0%) | 3 (3%) | 27 (26%) | 11 (35%) | |
| 6 | 68 (100%) | 1 (1%) | 16 (15%) | 3 (10%) | |
| Braak NFT stage | | | | | <0.0001 |
| B1 | 40 (59%) | 0 (0%) | 0 (0%) | 6 (19%) | |
| B2 | 25 (37%) | 1 (1%) | 4 (4%) | 20 (65%) | |
| B3 | 3 (4%) | 89 (99%) | 100 (96%) | 5 (16%) | |
| CERAD score | | | | | <0.0001 |
| C0 | 56 (82%) | 1 (1%) | 0 (0%) | 23 (74%) | |
| C1 | 8 (12%) | 8 (9%) | 4 (4%) | 8 (26%) | |
| C2 | 4 (6%) | 22 (24%) | 34 (33%) | 0 (0%) | |
| C3 | 0 (0%) | 59 (66%) | 66 (63%) | 0 (0%) | |
| Vascular score | | | | | 0.0009 |
| 0 | 57 (84%) | | | | |

*(continued on next page)*

**Table 1** (*continued*)

|  | FTLD-TDP Types A-C n = 68 | AD-TDP Type β n = 90 | AD-TDP Type α n = 104 | Pure-TDP Type α n = 31 | p-value |
|---|---|---|---|---|---|
|  |  | 50 (56%) | 53 (51%) | 20 (65%) |  |
| 1 | 4 (6%) | 7 (8%) | 9 (9%) | 2 (6%) |  |
| 2 | 7 (10%) | 22 (24%) | 36 (35%) | 8 (26%) |  |
| 3 | 0 (0%) | 11 (12%) | 6 (6%) | 1 (3%) |  |
| ADNC likelihood |  |  |  |  | <0.0001 |
| None | 55 (81%) | 0 (0%) | 0 (0%) | 23 (74%) |  |
| Low | 13 (19%) | 0 (0%) | 0 (0%) | 8 (26%) |  |
| Intermediate | 0 (0%) | 32 (36%) | 42 (40%) | 0 (0%) |  |
| High | 0 (0%) | 58 (64%) | 62 (60%) | 0 (0%) |  |
| LBD stage |  |  |  |  | <0.0001 |
| 0 | 67 (99%) | 49 (54%) | 56 (54%) | 22 (71%) |  |
| 1 | 0 (0%) | 0 (0%) | 2 (2%) | 3 (10%) |  |
| 2 | 1 (1%) | 21 (23%) | 22 (21%) | 3 (10%) |  |
| 3 | 0 (0%) | 20 (22%) | 24 (23%) | 3 (10%) |  |

Summaries are mean (SD) for continuous variables, *n (%)* for categorical variables.
*P*-values are from ANOVA or Kruskal-Wallis tests for continuous variables depending on distribution and from Chi-squared test for categorical variables.
  [a] summary is represented as median (interquartile range).

### 3.2.2. Hippocampus

Young FTLD-TDP started off with larger volumes of the hippocampus 10 years before death, but show similar rates of atrophy, compared to old FTLD-TDP. AD-TDP type-α showed similar volume estimates to older FTLD-TDP patients 10 years before death with both groups having the smallest volumes; by the time of death FTLD-TDP (both ages) showed smaller volumes than all other TDP groups. AD-TDP type-β and pure-TDP showed larger volumes compared to AD-TDP type-α across the disease course, with volume differences increasing close to death. Young FTLD-TDP showed similar volumes 10 years before death to AD-TDP type-β and pure-TDP.

### 3.2.3. Temporal pole

Old FTLD-TDP had the smallest volumes of the temporal pole across all time points. Rates of atrophy did not differ between old and young FTLD-TDP. AD-TDP type-α had smaller volumes than AD-TDP type-β 10 years before death, but with similar rates of atrophy. By death, all groups were different, with pure-TDP having the largest volumes, followed by AD-TDP type-β, AD-TDP type-α, young FTLD-TDP and then old FTLD-TDP.

### 3.2.4. Inferior temporal lobe

Young and old FTLD-TDP had the fastest rates of atrophy in the inferior temporal lobe with smaller volumes close to death compared to all other groups. In AD-TDP cases, those with type-α had smaller volumes at all time points compared to those with type-β, with similar rates of atrophy. Pure-TDP had slower rates of atrophy compared to all other groups and largest volumes close to death.

### 3.2.5. Middle frontal gyrus

Volumes of the middle frontal gyrus were comparable across groups ten years from death. However, rates of atrophy were faster in young FTLD-TDP compared to all other groups, including old FTLD-TDP (Supplementary Fig. 3), and hence young FTLD-TDP had the smallest volumes close to death. Old FTLD-TDP had the next fastest rates of atrophy and had smaller volumes close to death compared to the AD-TDP groups and pure-TDP. Pure-TDP had larger volumes close to death compared to all groups, except AD-TDP type-α.

### 3.2.6. Influence of age

The influence of age on these models is highlighted in Supplementary Fig. 2. Within FTLD-TDP, older age at death was associated with smaller hippocampal, temporal pole, and inferior temporal volumes and larger middle frontal volumes, but slower rate of atrophy only in the middle frontal gyrus with similar rates of atrophy across other regions. Within non FTLD-TDP cases, younger age at death was associated with smaller amygdala, hippocampal, inferior temporal, and middle frontal volumes, and faster rates of atrophy in all regions.

In the middle frontal gyrus volume differences between young FTLD-TDP individuals and non FTLD-TDP groups could be due to smaller volumes in younger individuals, faster atrophy in younger individuals, or a combination of the two (if there is no difference between older FTLD-TDP individuals and the other groups). In all other regions, where there is no FTLD-TDP age gradient in atrophy rate, if there is a difference between young FTLD-TDP and non FTLD-TDP groups but not between older FTLD-TDP and non FTLD-TDP groups, the difference is likely due to the age shifting cross-sectional volume in the younger FTLD-TDP individuals.
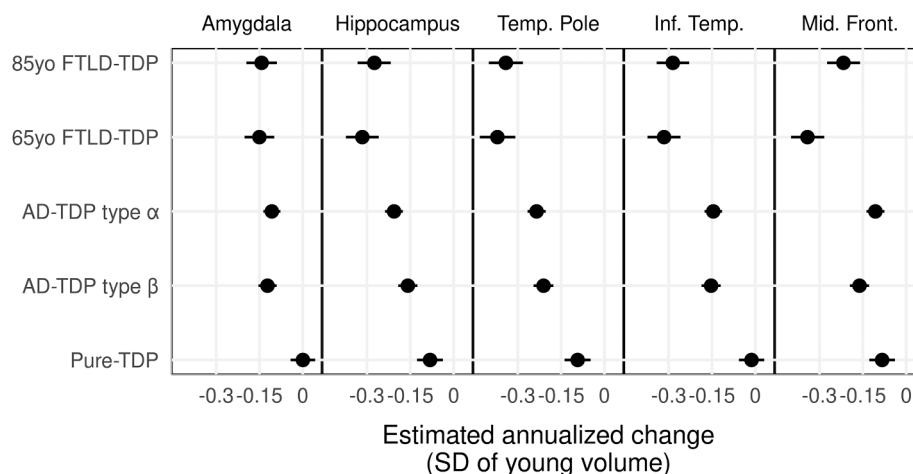


**Fig. 1.** Forest plot showing estimates and 90% confidence intervals for longitudinal effects on estimated annualized change in brain volume of patients with TDP-43 compared to healthy controls. Forest plots that do not cross grey line at 0 represent evidence of a nonzero rate of atrophy posterior probability > 0.90).

**Table 2**
Intergroup comparison of longitudinal effects.

| region | First | Second | Median difference | P(First > Second) | P(Second > First) |
| --- | --- | --- | --- | --- | --- |
| Amygdala | 65yo FTLD-TDP | 85yo FTLD-TDP | −0.01 | 0.445 | 0.555 |
|  | 65yo FTLD-TDP | pure-TDP | −0.15 | 0.002 | 0.998 |
|  | 65yo FTLD-TDP | AD-TDP type α | −0.04 | 0.173 | 0.827 |
|  | 65yo FTLD-TDP | AD-TDP type β | −0.03 | 0.274 | 0.726 |
|  | 85yo FTLD-TDP | pure-TDP | −0.14 | 0.003 | 0.997 |
|  | 85yo FTLD-TDP | AD-TDP type α | −0.04 | 0.223 | 0.777 |
|  | 85yo FTLD-TDP | AD-TDP type β | −0.02 | 0.336 | 0.664 |
|  | pure-TDP | AD-TDP type α | 0.11 | 0.998 | 0.002 |
|  | pure-TDP | AD-TDP type β | 0.12 | 0.999 | 0.001 |
|  | AD-TDP type α | AD-TDP type β | 0.02 | 0.720 | 0.280 |
| Hippocampus | 65yo FTLD-TDP | 85yo FTLD-TDP | −0.04 | 0.255 | 0.745 |
|  | 65yo FTLD-TDP | pure-TDP | −0.23 | <0.001 | >0.999 |
|  | 65yo FTLD-TDP | AD-TDP type α | −0.11 | 0.015 | 0.985 |
|  | 65yo FTLD-TDP | AD-TDP type β | −0.16 | 0.001 | 0.999 |
|  | 85yo FTLD-TDP | pure-TDP | −0.19 | <0.001 | >0.999 |
|  | 85yo FTLD-TDP | AD-TDP type α | −0.07 | 0.084 | 0.916 |
|  | 85yo FTLD-TDP | AD-TDP type β | −0.12 | 0.010 | 0.990 |
|  | pure-TDP | AD-TDP type α | 0.13 | 0.999 | 0.001 |
|  | pure-TDP | AD-TDP type β | 0.08 | 0.970 | 0.030 |
|  | AD-TDP type α | AD-TDP type β | −0.05 | 0.038 | 0.962 |
| Temp. Pole | 65yo FTLD-TDP | 85yo FTLD-TDP | −0.03 | 0.329 | 0.671 |
|  | 65yo FTLD-TDP | pure-TDP | −0.28 | <0.001 | >0.999 |
|  | 65yo FTLD-TDP | AD-TDP type α | −0.14 | 0.005 | 0.995 |
|  | 65yo FTLD-TDP | AD-TDP type β | −0.16 | 0.002 | 0.998 |
|  | 85yo FTLD-TDP | pure-TDP | −0.25 | <0.001 | >0.999 |
|  | 85yo FTLD-TDP | AD-TDP type α | −0.11 | 0.018 | 0.982 |
|  |  |  | −0.13 | 0.006 | 0.994 |

**Table 2** (*continued*)

| region | First | Second | Median difference | P(First > Second) | P(Second > First) |
| --- | --- | --- | --- | --- | --- |
|  | 85yo FTLD-TDP | AD-TDP type β |  |  |  |
|  | pure-TDP | AD-TDP type α | 0.14 | >0.999 | <0.001 |
|  | pure-TDP | AD-TDP type β | 0.12 | 0.997 | 0.003 |
|  | AD-TDP type α | AD-TDP type β | −0.02 | 0.191 | 0.809 |
| Inf. Temp. | 65yo FTLD-TDP | 85yo FTLD-TDP | −0.03 | 0.307 | 0.693 |
|  | 65yo FTLD-TDP | pure-TDP | −0.3 | <0.001 | >0.999 |
|  | 65yo FTLD-TDP | AD-TDP type α | −0.17 | <0.001 | >0.999 |
|  | 65yo FTLD-TDP | AD-TDP type β | −0.16 | 0.001 | 0.999 |
|  | 85yo FTLD-TDP | pure-TDP | −0.27 | <0.001 | >0.999 |
|  | 85yo FTLD-TDP | AD-TDP type α | −0.14 | 0.002 | 0.998 |
|  | 85yo FTLD-TDP | AD-TDP type β | −0.13 | 0.003 | 0.997 |
|  | pure-TDP | AD-TDP type α | 0.13 | >0.999 | <0.001 |
|  | pure-TDP | AD-TDP type β | 0.14 | >0.999 | <0.001 |
|  | AD-TDP type α | AD-TDP type β | 0.01 | 0.611 | 0.389 |
| Mid. Front. | 65yo FTLD-TDP | 85yo FTLD-TDP | −0.12 | 0.022 | 0.978 |
|  | 65yo FTLD-TDP | pure-TDP | −0.26 | <0.001 | >0.999 |
|  | 65yo FTLD-TDP | AD-TDP type α | −0.24 | <0.001 | >0.999 |
|  | 65yo FTLD-TDP | AD-TDP type β | −0.18 | <0.001 | >0.999 |
|  | 85yo FTLD-TDP | pure-TDP | −0.13 | 0.008 | 0.992 |
|  | 85yo FTLD-TDP | AD-TDP type α | −0.11 | 0.012 | 0.988 |
|  | 85yo FTLD-TDP | AD-TDP type β | −0.06 | 0.140 | 0.860 |
|  | pure-TDP | AD-TDP type α | 0.02 | 0.737 | 0.263 |
|  | pure-TDP | AD-TDP type β | 0.08 | 0.973 | 0.027 |
|  | AD-TDP type α | AD-TDP type β | 0.06 | 0.979 | 0.021 |

## 4. Discussion

In this study we compare the patterns, degree, and rates of regional brain atrophy in FTLD-TDP versus non-FTLD AD-TDP (type-α and β) and pure-TDP. All pathologic variants of TDP-43 proteinopathy were associated with increased rates of atrophy in the hippocampus, temporal pole, and middle frontal gyrus with FTLD-TDP and AD-TDP also associated with increased rates of atrophy in the inferior temporal lobe and amygdala. While rates of atrophy in FTLD-TDP were faster than at least
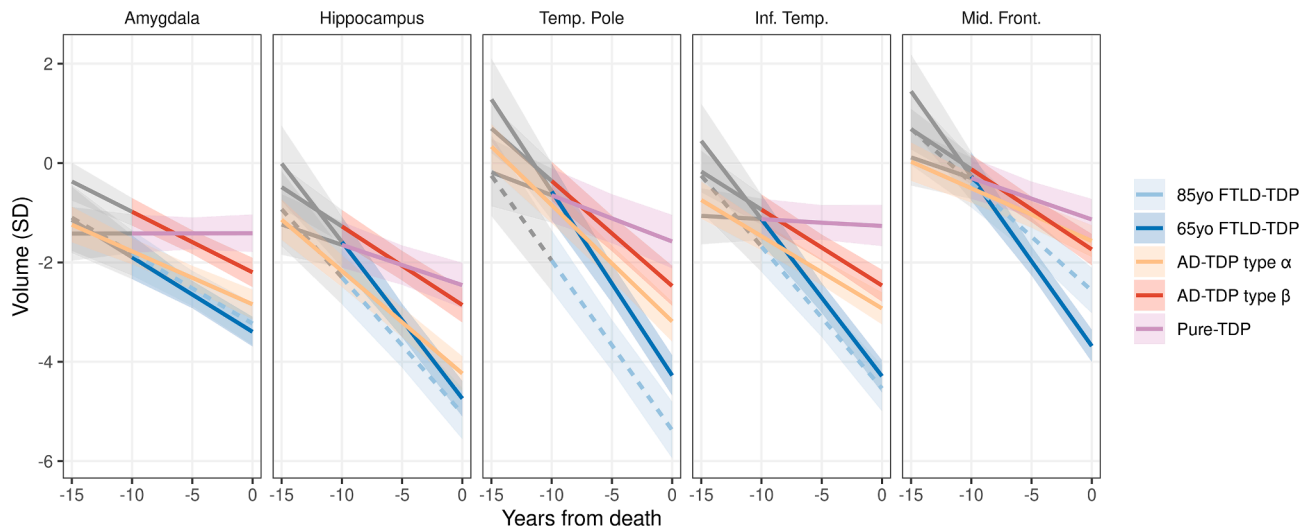
**Fig. 2.** Fitted curves showing the relationship between rates of atrophy and regional volumes on the time continuum for the TDP-43 pathologic groups. Covariates are set to reference levels showing the fits for an 85-year-old-at-death female with vascular score 0 and LBD score 0 on a 1.5 T MRI, except for 65-yo FTLD group. Fits are showing rate-volume relationship 10 years prior to death in all groups besides AD-TDP type α where sufficient data are available at 15 years prior to death. Shaded in grey fitted curves for −15 to −10 time period reflect scarce data.

some of the non-FTLD groups in all regions, the inferior temporal lobe and temporal pole were the regions that best distinguished FTLD-TDP from all non-FTLD TDP-43 groups. The rate of atrophy in the frontal lobe, however, was modulated by age with younger FTLD-TDP having faster rates than old FTLD-TDP. In the FTLD-TDP patients, the hippocampus was not spared relative to cortical regions. AD-TDP type-α was associated with smaller volumes across the disease course than AD-TDP type-β in the amygdala, hippocampus, and inferior temporal lobe, although AD-TDP type-α only showed faster rates in the hippocampus. Pure-TDP showed the slowest rates of atrophy and largest volumes close to death across most regions. Interestingly, rates of hippocampal, amygdala and middle frontal atrophy were similar between old FTLD-TDP and some subgroups of non-FTLD TDP-43 types.

Here we further our earlier findings by identifying similarities and differences in rates and trajectories of regional brain atrophy between non-FTLD TDP-43 types and most importantly how they compare to FTLD-TDP. Consistent with, and complementary to, our prior work (Josephs et al., 2020), AD-TDP type-α showed greater atrophy rates of the hippocampus compared to the inferior temporal and middle frontal gyri throughout the last 10 years before death. We also assessed the amygdala and temporal pole in this study and now add to the literature showing that they also have increased rates of atrophy to a greater degree than the frontal cortex in AD-TDP type-α. Similarly, old FTLD-TDP showed greater atrophy in the hippocampus compared to the frontal lobe and had comparable hippocampal volumes at death and rates of hippocampal atrophy to AD-TDP. These findings support several conclusions. First, hippocampal atrophy, often considered a hallmark of AD, is also a prominent feature of FTLD-TDP and can be even more prominent than AD-associated hippocampal atrophy (Barnes et al., 2006). Second, older age in FTLD-TDP patients is associated with a limbic-predominant pattern of atrophy with relatively spared middle frontal gyrus which is consistent with the pattern of TDP-43 deposition in older genetically confirmed FTLD-TDP patients (Buciuc et al., 2021b). This relationship between young/old and cortical/limbic is reminiscent of the relationship of atrophy in young versus old onset AD (Whitwell et al., 2012a). This association of old FTLD-TDP with relative sparing of the frontal lobe might translate into a different, likely amnestic, clinical phenotype for older FTLD-TDP patients compared to young FTLD patients. Clinicians should, therefore, consider broadening the differential diagnosis to include FTLD-TDP in older patients with an amnestic syndrome (Buciuc et al., 2021b; Seo et al., 2018).

The biggest difference in rates of atrophy between FTLD and non-FTLD cases, regardless of age and TDP type, was observed in the inferior temporal lobe and temporal pole; suggesting these regions are particularly associated with what we currently define as FTLD-TDP. Rates of atrophy in these two regions did not change with age in FTLD-TDP, although volume of the temporal pole was smaller in older FTLD-TDP patients. This concurs with a study assessing typical young FTLD-TDP patients who had more cortical pathology than non-FTLD TDP-43 patients (Robinson et al., 2020). The inferior temporal lobe and temporal pole are typically atrophic in FTLD-TDP cases, including in patients with progranulin and *C9ORF72* mutations (Whitwell et al., 2015; Whitwell et al., 2012b) which was common in this cohort, whereas atrophy of the medial temporal lobe is a predominant feature of FTLD-TDP type C (Rohrer et al., 2010; Whitwell et al., 2010) that was rare in our cohort. Our finding also complements another study where inferior temporal lobe had the highest rate of longitudinal change in volume in a cohort of patients with frontotemporal dementia (FTD) spectrum diagnosis (Pankov et al., 2016). In this study the inferior temporal lobe was also reported as an overlapping atrophy region for different FTD phenotypes which makes our finding more generalizable given that our FTLD-TDP cohort is heterogeneous in terms of TDP-43 morphological types, genetics, and clinical presentations.

The FTLD-TDP patients had faster rates of middle frontal gyrus atrophy compared to the non-FTLD-TDP patients. This was somewhat expected since the presence of frontal degeneration at autopsy was a feature utilized in the diagnosis of FTLD-TDP. However, this difference in rates was age dependent. That is, typical (young) FTLD-TDP patients had faster rates of atrophy in the middle frontal gyrus compared to older FTLD-TDP and showed more striking differences from non-FTLD TDP-43. Both young and old FTLD-TDP also had smaller frontal volumes at death compared to the non-FTLD TDP-43 groups. Since all the FTLD-TDP cases had TDP-43 deposited in the frontal cortex compared to ≤15% of the AD-TDP and pure-TDP cases it is not surprising that the middle frontal gyrus was a more vulnerable region to FTLD-TDP. The central question is why the vulnerability of this brain region changes with age in FTLD. One explanation could be that the burden of TDP-43 pathology in the frontal cortex is greater in young FTLD patients, whereas TDP burden is limbic predominant in old age FTLD, as it was observed in an independent cohort, similar to what is observed in AD (Buciuc et al., 2021b; Murray et al., 2011; Whitwell et al., 2012a). Although younger age was associated with faster frontal atrophy it was

**Table 3**
Probability of differences in fitted volumes at −10 and 0 years before death.

| Timescale | Region | First | Second | Median difference | P(First > Second) | P(Second > First) |
|---|---|---|---|---|---|---|
| −10 years prior to death | Amygdala | 65yo FTLD-TDP | 85yo FTLD-TDP | −0.09 | 0.570 | 0.430 |
| | | 65yo FTLD-TDP | pure-TDP | −0.48 | 0.862 | 0.138 |
| | | 65yo FTLD-TDP | AD-TDP type α | −0.12 | 0.626 | 0.374 |
| | | 65yo FTLD-TDP | AD-TDP type β | −0.91 | 0.990 | 0.010 |
| | | 85yo FTLD-TDP | pure-TDP | −0.39 | 0.803 | 0.197 |
| | | 85yo FTLD-TDP | AD-TDP type α | −0.04 | 0.538 | 0.462 |
| | | 85yo FTLD-TDP | AD-TDP type β | −0.83 | 0.982 | 0.018 |
| | | pure-TDP | AD-TDP type α | 0.35 | 0.130 | 0.870 |
| | | pure-TDP | AD-TDP type β | −0.44 | 0.906 | 0.094 |
| | | AD-TDP type α | AD-TDP type β | −0.80 | >0.999 | <0.001 |
| | Hippocampus | 65yo FTLD-TDP | 85yo FTLD-TDP | 0.71 | 0.100 | 0.900 |
| | | 65yo FTLD-TDP | pure-TDP | 0.06 | 0.454 | 0.546 |
| | | 65yo FTLD-TDP | AD-TDP type α | 0.58 | 0.090 | 0.910 |
| | | 65yo FTLD-TDP | AD-TDP type β | −0.31 | 0.757 | 0.243 |
| | | 85yo FTLD-TDP | pure-TDP | −0.65 | 0.884 | 0.116 |
| | | 85yo FTLD-TDP | AD-TDP type α | −0.13 | 0.608 | 0.392 |
| | | 85yo FTLD-TDP | AD-TDP type β | −1.03 | 0.984 | 0.016 |
| | | pure-TDP | AD-TDP type α | 0.52 | 0.079 | 0.921 |
| | | pure-TDP | AD-TDP type β | −0.37 | 0.819 | 0.181 |
| | | AD-TDP type α | AD-TDP type β | −0.90 | >0.999 | <0.001 |
| | Temp. Pole | 65yo FTLD-TDP | 85yo FTLD-TDP | 1.39 | 0.013 | 0.987 |
| | | 65yo FTLD-TDP | pure-TDP | 0.08 | 0.446 | 0.554 |
| | | 65yo FTLD-TDP | AD-TDP type α | 0.27 | 0.290 | 0.710 |
| | | 65yo FTLD-TDP | AD-TDP type β | −0.21 | 0.656 | 0.344 |
| | | 85yo FTLD-TDP | pure-TDP | −1.32 | 0.982 | 0.018 |
| | | 85yo FTLD-TDP | AD-TDP type α | −1.12 | 0.981 | 0.019 |
| | | 85yo FTLD-TDP | AD-TDP type β | −1.60 | 0.998 | 0.002 |
| | | pure-TDP | AD-TDP type α | 0.19 | 0.332 | 0.668 |
| | | pure-TDP | AD-TDP type β | −0.28 | 0.731 | 0.269 |
| | | AD-TDP type α | AD-TDP type β | −0.48 | 0.935 | 0.065 |
| | Inf. Temp. | 65yo FTLD-TDP | 85yo FTLD-TDP | 0.54 | 0.146 | 0.854 |
| | | 65yo FTLD-TDP | pure-TDP | 0.00 | 0.502 | 0.498 |
| | | 65yo FTLD-TDP | AD-TDP type α | 0.34 | 0.205 | 0.794 |
| | | 65yo FTLD-TDP | AD-TDP type β | −0.19 | 0.672 | 0.328 |
| | | 85yo FTLD-TDP | pure-TDP | −0.55 | 0.868 | 0.132 |
| | | 85yo FTLD-TDP | AD-TDP type α | −0.21 | 0.685 | 0.315 |
| | | 85yo FTLD-TDP | AD-TDP type β | −0.75 | 0.958 | 0.042 |
| | | pure-TDP | AD-TDP type α | 0.34 | 0.159 | 0.841 |
| | | pure-TDP | AD-TDP type β | −0.20 | 0.708 | 0.292 |
| | | AD-TDP type α | AD-TDP type β | −0.53 | 0.984 | 0.016 |
| | Mid. Front. | 65yo FTLD-TDP | 85yo FTLD-TDP | 0.13 | 0.403 | 0.597 |
| | | 65yo FTLD-TDP | pure-TDP | 0.04 | 0.471 | 0.529 |
| | | 65yo FTLD-TDP | AD-TDP type α | 0.24 | 0.286 | 0.714 |
| | | 65yo FTLD-TDP | AD-TDP type β | −0.14 | 0.632 | 0.368 |
| | | 85yo FTLD-TDP | pure-TDP | −0.09 | 0.574 | 0.426 |
| | | 85yo FTLD-TDP | AD-TDP type α | 0.11 | 0.402 | 0.598 |
| | | 85yo FTLD-TDP | AD-TDP type β | −0.27 | 0.734 | 0.266 |
| | | pure-TDP | AD-TDP type α | 0.20 | 0.278 | 0.722 |
| | | pure-TDP | AD-TDP type β | −0.18 | 0.692 | 0.308 |
| | | AD-TDP type α | AD-TDP type β | −0.38 | 0.939 | 0.061 |
| 0 years prior to death | Amygdala | 65yo FTLD-TDP | 85yo FTLD-TDP | −0.16 | 0.699 | 0.301 |
| | | 65yo FTLD-TDP | pure-TDP | −1.98 | >0.999 | <0.001 |
| | | 65yo FTLD-TDP | AD-TDP type α | −0.55 | 0.967 | 0.033 |
| | | 65yo FTLD-TDP | AD-TDP type β | −1.20 | >0.999 | <0.001 |
| | | 85yo FTLD-TDP | pure-TDP | −1.82 | >0.999 | <0.001 |
| | | 85yo FTLD-TDP | AD-TDP type α | −0.39 | 0.850 | 0.150 |
| | | 85yo FTLD-TDP | AD-TDP type β | −1.03 | 0.997 | 0.003 |
| | | pure-TDP | AD-TDP type α | 1.43 | < 0.001 | >0.999 |
| | | pure-TDP | AD-TDP type β | 0.78 | 0.009 | 0.991 |
| | | AD-TDP type α | AD-TDP type β | −0.65 | 0.995 | 0.005 |
| | Hippocampus | 65yo FTLD-TDP | 85yo FTLD-TDP | 0.30 | 0.214 | 0.786 |
| | | 65yo FTLD-TDP | pure-TDP | −2.28 | >0.999 | <0.001 |
| | | 65yo FTLD-TDP | AD-TDP type α | −0.51 | 0.920 | 0.080 |
| | | 65yo FTLD-TDP | AD-TDP type β | −1.89 | >0.999 | <0.001 |
| | | 85yo FTLD-TDP | pure-TDP | −2.58 | >0.999 | <0.001 |
| | | 85yo FTLD-TDP | AD-TDP type α | −0.81 | 0.963 | 0.037 |
| | | 85yo FTLD-TDP | AD-TDP type β | −2.19 | >0.999 | <0.001 |
| | | pure-TDP | AD-TDP type α | 1.77 | <0.001 | >0.999 |
| | | pure-TDP | AD-TDP type β | 0.40 | 0.164 | 0.836 |
| | | AD-TDP type α | AD-TDP type β | −1.38 | >0.999 | <0.001 |
| | Temp. Pole | 65yo FTLD-TDP | 85yo FTLD-TDP | 1.10 | 0.006 | 0.994 |
| | | 65yo FTLD-TDP | pure-TDP | −2.70 | > 0.999 | <0.001 |
| | | 65yo FTLD-TDP | AD-TDP type α | −1.09 | 0.996 | 0.004 |
| | | 65yo FTLD-TDP | AD-TDP type β | −1.81 | >0.999 | <0.001 |

**Table 3** (*continued*)

| Timescale | Region | First | Second | Median difference | P(First > Second) | P(Second > First) |
|---|---|---|---|---|---|---|
| | | 85yo FTLD-TDP | pure-TDP | −3.80 | >0.999 | <0.001 |
| | | 85yo FTLD-TDP | AD-TDP type α | −2.18 | >0.999 | <0.001 |
| | | 85yo FTLD-TDP | AD-TDP type β | −2.90 | >0.999 | <0.001 |
| | | pure-TDP | AD-TDP type α | 1.61 | <0.001 | >0.999 |
| | | pure-TDP | AD-TDP type β | 0.89 | 0.030 | 0.970 |
| | | AD-TDP type α | AD-TDP type β | −0.72 | 0.986 | 0.014 |
| | Inf. Temp. | 65yo FTLD-TDP | 85yo FTLD-TDP | 0.25 | 0.236 | 0.764 |
| | | 65yo FTLD-TDP | pure-TDP | −3.03 | >0.999 | <0.001 |
| | | 65yo FTLD-TDP | AD-TDP type α | −1.37 | >0.999 | <0.001 |
| | | 65yo FTLD-TDP | AD-TDP type β | −1.83 | >0.999 | <0.001 |
| | | 85yo FTLD-TDP | pure-TDP | −3.28 | >0.999 | <0.001 |
| | | 85yo FTLD-TDP | AD-TDP type α | −1.61 | >0.999 | <0.001 |
| | | 85yo FTLD-TDP | AD-TDP type β | −2.07 | >0.999 | <0.001 |
| | | pure-TDP | AD-TDP type α | 1.66 | <0.001 | >0.999 |
| | | pure-TDP | AD-TDP type β | 1.21 | 0.001 | >0.999 |
| | | AD-TDP type α | AD-TDP type β | −0.46 | 0.962 | 0.038 |
| | Mid. Front. | 65yo FTLD-TDP | 85yo FTLD-TDP | −1.12 | 0.999 | 0.001 |
| | | 65yo FTLD-TDP | pure-TDP | −2.54 | >0.999 | <0.001 |
| | | 65yo FTLD-TDP | AD-TDP type α | −2.11 | >0.999 | <0.001 |
| | | 65yo FTLD-TDP | AD-TDP type β | −1.94 | >0.999 | <0.001 |
| | | 85yo FTLD-TDP | pure-TDP | −1.43 | 0.999 | 0.001 |
| | | 85yo FTLD-TDP | AD-TDP type α | −1.00 | 0.992 | 0.008 |
| | | 85yo FTLD-TDP | AD-TDP type β | −0.83 | 0.977 | 0.023 |
| | | pure-TDP | AD-TDP type α | 0.44 | 0.112 | 0.888 |
| | | pure-TDP | AD-TDP type β | 0.61 | 0.054 | 0.946 |
| | | AD-TDP type α | AD-TDP type β | 0.17 | 0.257 | 0.743 |

also associated with longer time from first scan to death ($r = −0.24$, $p = 0.045$), and hence we do not see a relationship between disease duration and age, with shorter disease occurring in younger FTLD-TDP patients.

While the presence of focal gross atrophy and microvacuolation defined the FTLD cases, non-FTLD pure-TDP represents an interesting group as TDP-43 is primarily the only pathological substrate in the brains of these patients. This group behaved quite differently, in terms of rates of atrophy, compared to the FTLD-TDP and AD-TDP groups. While hippocampus was the most atrophied region in pure-TDP and was comparable in volume to young FTLD-TDP and AD-TDP type-β 10 years before death, the rates of atrophy were much slower in pure-TDP. In fact, rates of atrophy were the slowest, and volumes at death largest, across all regions in pure-TDP. This may be partially attributable to the fact that almost a third of the cases in pure-TDP group had TDP-43 deposition limited to the amygdala (Stage 1), therefore, it is not unexpected that the volumes of hippocampus, inferior temporal and frontal regions would be relatively spared in these cases. The hippocampus being the most affected region in this group of patients may be explained by the fact that ~40% of patients had TDP-43 deposition restricted to limbic regions compared to FTLD-TDP with diffuse TDP-43 aggregation involving frontal cortices. The volumes and rates of atrophy of the middle frontal region were similar between pure-TDP and AD-TDP type-α perhaps reflecting the fact that a similar proportion of cases had frontal TDP-43 inclusions. Considering the above, it is tempting to conclude that non-FTLD pure-TDP has a different pathobiology from FTLD-TDP and AD-TDP. More work is certainly needed on this group, especially since the vast majority were cognitively normal at the time of death..

In addition to similarities and differences between FTLD and non-FTLD TDP-43 pathologic variants, one of the novelties of this study is the identification of differences in the pattern and rates of neurodegeneration between AD-TDP type-α and β which adds to already identified genetic, clinical, demographic, molecular and pathologic distinctions between them (Buciuc et al., 2020c; Josephs et al., 2019b; Tomé et al., 2020). We observed the biggest differences by type in the hippocampus with smaller volumes and faster rates of atrophy in AD-TDP type-α compared to type-β which is consistent with our original study on TDP-43 types (Josephs et al., 2019b). This difference in rate could be related to TDP-43 stage, since type-α, as expected, had a higher percentage of cases with advanced stages of TDP-43 deposition (Josephs et al., 2019b), and higher TDP-43 stage is associated with faster atrophy

rates (Josephs et al., 2017; Josephs et al., 2020). Importantly, the AD-TDP type-α and -β groups were well matched in regards the severity of AD pathology. We also found smaller volumes of the amygdala, temporal pole, and inferior temporal lobe in type-α compared to type-β throughout the disease, although rates of atrophy in these regions did not differ between types. This may suggest these regions are affected early in the disease course with little pathological progression in contrast to the hippocampus which progressively worsens over time in type-α. On the contrary, we found evidence suggesting that AD-TDP type-β have faster rates of atrophy in the middle frontal gyrus than type-α which validates our previous finding of an association between TDP-43 type-β, but not type-α, and smaller superior frontal volumes compared to controls (Josephs et al., 2019b). Hence, once again we observe this propensity for AD-TDP type-β to have faster rates of frontal lobe atrophy than type-α, despite the fact that TDP-43 deposition in the frontal lobe is not a common feature of AD-TDP type-β and more often a feature of type-α. One explanation for this finding could be that faster rates of atrophy occur at different timepoints for type-α and type-β. If we take a closer look at the rates of atrophy and volumes 10 years prior to death, we can see that AD-TDP type-α patients start off with smaller volumes in all analyzed regions suggesting that some atrophy has already occurred by this point in time. We do not see any difference in volumes of middle frontal gyrus at the different time points analyzed, however the gap between volumes is in fact larger 15 years prior to death. Hence, it seems to be the case that due to faster rates of atrophy later in the disease for type-β, type-β "catches up" in volume loss to type-α in the last decade prior to death. This is not surprising, given that we previously demonstrated in our earlier work that TDP-43-associated rates of brain atrophy are non-linear (Josephs et al., 2020). A second possibility, for this observation could be that we are not accounting for the added effects of one of more TDP-43 regulated proteins. One such protein, for example, is stathmin-2 whose expression is regulated by TDP-43 (Melamed et al., 2019) with truncated stathmin-2 being strongly linked to FTLD-TDP and FTLD-ALS (Melamed et al., 2019; Prudencio et al., 2020). Little is known about stathmin-2 in AD-TDP. Regardless, it appears that AD-TDP type-α targets the hippocampus and temporal lobe resulting in faster rate and degree of atrophy, whereas AD-TDP type-β might be associated with late accelerated neurodegeneration in the frontal regions.

The strengths of our study are the longitudinal design, large number

of autopsy-confirmed cases, available MRI scans and robust statistical analysis. Whereas we subtyped non-FTLD TDP cases in those with/without ADNC and types-α and β to assess for differences in rates of atrophy, our FTLD-TDP cohort was imbalanced across types A, B and C and therefore didn't have the degrees of freedom necessary to include terms for FTLD-TDP subtype which could be a limitation. Another limitation was the fact that scans were obtained from multiple scanners at both 1.5 T and 3 T field strengths. However, we included field strength as a fixed effect in the hierarchical model to account for this potential bias. Again, while we did not have the degrees of freedom to account for all scanners, the model includes random effects per person to implicitly account for potential biases that are not explicitly specified in the model, and hence protect against such bias. The control cohort used to convert regional volumes to W-scores were all performed at 3 T which may have introduced some additional bias, although again the model should be managing this bias. Since, by definition, non-FTLD TDP-43 type-β needs to co-exist with tau NFTs, the absence of pure-TDP cases with type-β inclusions in our cohort is not a bias but rather a natural phenomenon.

Lastly, we did not assess for associations between the specific TDP-43 inclusions (e.g., neuronal cytoplasmic inclusions, dystrophic neurites and intranuclear inclusions), or the burden or distribution of TDP-43 across regions, and the rates and patterns of atrophy.

There are several implications of our findings that can be useful to the field, particularly for the classification and clinical diagnosis of TDP-43 proteinopathies. Given the evidence of differences in the patterns and rates of atrophy among FTLD-TDP, AD-TDP and pure-TDP it is justifiable to treat them separately, especially in clinical trials utilizing imaging as an outcome measure once *in vivo* biomarkers of TDP-43 deposition become available. The current study also emphasizes the importance of age in diagnosis and surveillance of FTLD-TDP patients. As current criteria for FTLD diagnosis are based on the findings in young patients (<65 years old at death), given the results of the present study, they do not appear to be generalizable to older patients. Therefore, a more limbic pattern of atrophy should not discourage an FTLD-TDP diagnosis, even in the presence, and especially in the absence, of AD (amyloid-β, tau) fluid or PET biomarkers. The findings could have clinical implications for prognosis since brain anatomy maps well onto clinical symptoms and different patterns of brain atrophy will likely translate into different patterns of clinical progression, although longitudinal clinical studies will be needed to test this hypothesis. Furthermore, the results have implications for treatment, stressing the importance of treatments targeting TDP-43 since treating the amyloid and tau may not be enough to prevent shrinkage of the brain. There is also the important issue of FTLD prevalence which may be vastly underestimated especially if other non-FTLD diagnositic labels are being applied to such cases. Lastly, age effects on the vulnerability of specific brain regions should be considered for the selection of age-appropriate MRI outcome measures for clinical treatment trials in FTLD-TDP.

*CRediT authorship contribution statement*

**Marina Buciuc:** Investigation, Writing – original draft. **Peter R. Martin:** Investigation, Methodology, Formal analysis, Visualization, Writing – review & editing. **Nirubol Tosakulwong:** Data curation, Writing – review & editing. **Melissa E. Murray:** Investigation, Writing – review & editing. **Leonard Petrucelli:** Resources, Writing – review & editing. **Matthew L. Senjem:** Software, Writing – review & editing. **Anthony J. Spychalla:** Software, Writing – review & editing. **David S. Knopman:** Investigation, Writing – review & editing. **Bradley F. Boeve:** Investigation, Writing – review & editing. **Ronald C. Petersen:** Investigation, Funding acquisition, Writing – review & editing. **Joseph E. Parisi:** Investigation, Writing – review & editing. **R. Ross Reichard:** Investigation, Writing – review & editing. **Dennis W. Dickson:** Investigation, Writing – review & editing. **Clifford R. Jack:** Resources, Funding acquisition, Writing – review & editing. **Jennifer L. Whitwell:** Investigation, Writing – review & editing. **Keith A. Josephs:**

Conceptualization, Investigation, Supervision, Funding acquisition, Writing – review & editing.

**Declaration of Competing Interest**

*Acknowledgement*

*Funding*

*Author contributions*

MB, JW and KJ contributed to concept and design of the study; MB, PRM, NT, MEM, LP, MLS, AJS, DSK, BFB, RCP, JEP, RRR, DWD, CRJ, JLW, and KJ contributed to the acquisition and analysis of data; MB, PRM, NT, JW, and KJ contributed to drafting the text and preparing the tables and figures. All authors revised the text for intellectual content.

**Appendix A. Supplementary data**

Supplementary data to this article can be found online at https://doi.org/10.1016/j.nicl.2022.102954.

**References**

Amador-Ortiz, C., Lin, W.L., Ahmed, Z., Personett, D., Davies, P., Duara, R., Graff-Radford, N.R., Hutton, M.L., Dickson, D.W., 2007. TDP-43 immunoreactivity in hippocampal sclerosis and Alzheimer's disease. Ann. Neurol. 61, 435–445.

Arai, T., Hasegawa, M., Akiyama, H., Ikeda, K., Nonaka, T., Mori, H., Mann, D., Tsuchiya, K., Yoshida, M., Hashizume, Y., 2006. TDP-43 is a component of ubiquitin-positive tau-negative inclusions in frontotemporal lobar degeneration and amyotrophic lateral sclerosis. Biochem. Biophys. Res. Commun. 351, 602–611.

Arai, T., Mackenzie, I.R., Hasegawa, M., Nonoka, T., Niizato, K., Tsuchiya, K., Iritani, S., Onaya, M., Akiyama, H., 2009. Phosphorylated TDP-43 in Alzheimer's disease and dementia with Lewy bodies. Acta Neuropathol. 117, 125–136.

Baker, M., Mackenzie, I.R., Pickering-Brown, S.M., Gass, J., Rademakers, R., Lindholm, C., Snowden, J., Adamson, J., Sadovnick, A.D., Rollinson, S., Cannon, A., Dwosh, E., Neary, D., Melquist, S., Richardson, A., Dickson, D., Berger, Z., Eriksen, J., Robinson, T., Zehr, C., Dickey, C.A., Crook, R., McGowan, E., Mann, D.,

Boeve, B., Feldman, H., Hutton, M., 2006. Mutations in progranulin cause tau-negative frontotemporal dementia linked to chromosome 17. Nature 442, 916–919.

Barnes, J., Whitwell, J.L., Frost, C., Josephs, K.A., Rossor, M., Fox, N.C., 2006. Measurements of the amygdala and hippocampus in pathologically confirmed Alzheimer disease and frontotemporal lobar degeneration. Arch. Neurol. 63, 1434–1439.

Bejanin, A., Murray, M.E., Martin, P., Botha, H., Tosakulwong, N., Schwarz, C.G., Senjem, M.L., Chetelat, G., Kantarci, K., Jack, C.R., Boeve, B.F., Knopman, D.S., Petersen, R.C., Giannini, C., Parisi, J.E., Dickson, D.W., Whitwell, J.L., Josephs, K.A., 2019. Antemortem volume loss mirrors TDP-43 staging in older adults with non-frontotemporal lobar degeneration. Brain 142, 3621–3635.

Braak, H., Alafuzoff, I., Arzberger, T., Kretzschmar, H., Del Tredici, K., 2006. Staging of Alzheimer disease-associated neurofibrillary pathology using paraffin sections and immunocytochemistry. Acta Neuropathol. 112, 389–404.

Brilleman, S.L., Crowther, M.J., Moreno-Betancur, M., Buros Novik, J., Dunyak, J., Al-Huniti, N., Fox, R., Hammerbacher, J., Wolfe, R., 2019. Joint longitudinal and time-to-event models for multilevel hierarchical data. Stat. Methods Med. Res. 28, 3502–3515.

Buciuc, M., Tosakulwong, N., Machulda, M.M., Whitwell, J.L., Weigand, S.D., Murray, M.E., Ross Reichard, R., Parisi, J.E., Dickson, D.W., Boeve, B.F., 2021a. TAR DNA-binding protein 43 is associated with rate of memory and functional and global cognitive decline in the decade prior to death. J. Alzheimers Dis. 1–11.

Buciuc, M., Wennberg, A.M., Weigand, S.D., Murray, M.E., Senjem, M.L., Spychalla, A.J., Boeve, B.F., Knopman, D.S., Jack Jr, C.R., Kantarci, K., 2020a. Effect modifiers of TDP-43 associated hippocampal atrophy rates in patients with alzheimer's disease neuropathological changes. J. Alzheimers Dis. 1–13.

Buciuc, M., Whitwell, J.L., Baker, M.C., Rademakers, R., Dickson, D.W., Josephs, K.A., 2021b. Old age genetically confirmed frontotemporal lobar degeneration with TDP-43 has limbic predominant TDP-43 deposition. Neuropathol. Appl. Neurobiol.

Buciuc, M., Whitwell, J.L., Boeve, B.F., Ferman, T.J., Graff-Radford, J., Savica, R., Kantarci, K., Fields, J.A., Knopman, D.S., Petersen, R.C., 2020b. TDP-43 is associated with a reduced likelihood of rendering a clinical diagnosis of dementia with Lewy bodies in autopsy-confirmed cases of transitional/diffuse Lewy body disease. J. Neurol. 1–10.

Buciuc, M., Whitwell, J.L., Tosakulwong, N., Weigand, S.D., Murray, M.E., Boeve, B.F., Knopman, D.S., Parisi, J.E., Petersen, R.C., Dickson, D.W., 2020c. Association between transactive response DNA-binding protein of 43 kDa type and cognitive resilience to Alzheimer's disease: a case-control study. Neurobiol. Aging 92, 92–97.

Cairns, N.J., Bigio, E.H., Mackenzie, I.R., Neumann, M., Lee, V.-M.-Y., Hatanpaa, K.J., White, C.L., Schneider, J.A., Grinberg, L.T., Halliday, G., 2007. Neuropathologic diagnostic and nosologic criteria for frontotemporal lobar degeneration: consensus of the Consortium for Frontotemporal Lobar Degeneration. Acta Neuropathol. 114, 5–22.

DeJesus-Hernandez, M., Mackenzie, I.R., Boeve, B.F., Boxer, A.L., Baker, M., Rutherford, N.J., Nicholson, A.M., Finch, N.A., Flynn, H., Adamson, J., Kouri, N., Wojtas, A., Sengdy, P., Hsiung, G.Y., Karydas, A., Seeley, W.W., Josephs, K.A., Coppola, G., Geschwind, D.H., Wszolek, Z.K., Feldman, H., Knopman, D.S., Petersen, R.C., Miller, B.L., Dickson, D.W., Boylan, K.B., Graff-Radford, N.R., Rademakers, R., 2011. Expanded GGGGCC hexanucleotide repeat in noncoding region of C9ORF72 causes chromosome 9p-linked FTD and ALS. Neuron 72, 245–256.

Fischl, B., Salat, D.H., Busa, E., Albert, M., Dieterich, M., Haselgrove, C., Van Der Kouwe, A., Killiany, R., Kennedy, D., Klaveness, S., 2002. Whole brain segmentation: automated labeling of neuroanatomical structures in the human brain. Neuron 33, 341–355.

Gelman, A., Hill, J., 2006. Data Analysis using Regression and Multilevel/Hierarchical Models. Cambridge University Press.

Goodrich, B., Gabry, J., Ali, I., Brilleman, S., 2020. rstanarm: Bayesian Applied Regression Modeling via Stan. R Package v. 2.19. 2.

Greenland, S., 2000. Principles of multilevel modelling. Int. J. Epidemiol. 29, 158–167.

Hasegawa, M., Arai, T., Akiyama, H., Nonaka, T., Mori, H., Hashimoto, T., Yamazaki, M., Oyanagi, K., 2007. TDP-43 is deposited in the Guam parkinsonism–dementia complex brains. Brain 130, 1386–1394.

Higashi, S., Iseki, E., Yamamoto, R., Minegishi, M., Hino, H., Fujisawa, K., Togo, T., Katsuse, O., Uchikado, H., Furukawa, Y., 2007. Concurrence of TDP-43, tau and α-synuclein pathology in brains of Alzheimer's disease and dementia with Lewy bodies. Brain Res. 1184, 284–294.

Hyman, B.T., Phelps, C.H., Beach, T.G., Bigio, E.H., Cairns, N.J., Carrillo, M.C., Dickson, D.W., Duyckaerts, C., Frosch, M.P., Masliah, E., 2012. National Institute on Aging–Alzheimer's Association guidelines for the neuropathologic assessment of Alzheimer's disease. Alzheimer's & Dementia 8, 1–13.

Hyman, B.T., Trojanowski, J.Q., 1997. Editorial on consensus recommendations for the postmortem diagnosis of Alzheimer disease from the National Institute on Aging and the Reagan Institute Working Group on diagnostic criteria for the neuropathological assessment of Alzheimer disease. J. Neuropathol. Exp. Neurol. 56, 1095.

Jack Jr, C.R., Lowe, V.J., Senjem, M.L., Weigand, S.D., Kemp, B.J., Shiung, M.M., Knopman, D.S., Boeve, B.F., Klunk, W.E., Mathis, C.A., 2008. 11C PiB and structural MRI provide complementary information in imaging of Alzheimer's disease and amnestic mild cognitive impairment. Brain 131, 665–680.

James, B.D., Wilson, R.S., Boyle, P.A., Trojanowski, J.Q., Bennett, D.A., Schneider, J.A., 2016. TDP-43 stage, mixed pathologies, and clinical Alzheimer's-type dementia. Brain 139, 2983–2993.

Josephs, K.A., Dickson, D.W., Tosakulwong, N., Weigand, S.D., Murray, M.E., Petrucelli, L., Liesinger, A.M., Senjem, M.L., Spychalla, A.J., Knopman, D.S., 2017. Rates of hippocampal atrophy and presence of post-mortem TDP-43 in patients with Alzheimer's disease: a longitudinal retrospective study. Lancet Neurol. 16, 917–924.

Josephs, K.A., Mackenzie, I., Frosch, M.P., Bigio, E.H., Neumann, M., Arai, T., Dugger, B. N., Ghetti, B., Grossman, M., Hasegawa, M., 2019a. LATE to the PART-y. Brain 142, e47.

Josephs, K.A., Martin, P.R., Weigand, S.D., Tosakulwong, N., Buciuc, M., Murray, M.E., Petrucelli, L., Senjem, M.L., Spychalla, A.J., Knopman, D.S., 2020. Protein contributions to brain atrophy acceleration in Alzheimer's disease and primary age-related tauopathy. Brain.

Josephs, K.A., Murray, M.E., Tosakulwong, N., Weigand, S.D., Serie, A.M., Perkerson, R. B., Matchett, B.J., Jack, C.R., Knopman, D.S., Petersen, R.C., 2019b. Pathological, imaging and genetic characteristics support the existence of distinct TDP-43 types in non-FTLD brains. Acta Neuropathol. 137, 227–238.

Josephs, K.A., Murray, M.E., Whitwell, J.L., Parisi, J.E., Petrucelli, L., Jack, C.R., Petersen, R.C., Dickson, D.W., 2014a. Staging TDP-43 pathology in Alzheimer's disease. Acta Neuropathol. 127, 441–450.

Josephs, K.A., Murray, M.E., Whitwell, J.L., Tosakulwong, N., Weigand, S.D., Petrucelli, L., Liesinger, A.M., Petersen, R.C., Parisi, J.E., Dickson, D.W., 2016. Updated TDP-43 in Alzheimer's disease staging scheme. Acta Neuropathol. 131, 571–585.

Josephs, K.A., Whitwell, J.L., Knopman, D.S., Hu, W.T., Stroh, D.A., Baker, M., Rademakers, R., Boeve, B.F., Parisi, J.E., Smith, G.E., Ivnik, R.J., Petersen, R.C., Jack Jr., C.R., Dickson, D.W., 2008. Abnormal TDP-43 immunoreactivity in AD modifies clinicopathologic and radiologic phenotype. Neurology 70, 1850–1857.

Josephs, K.A., Whitwell, J.L., Tosakulwong, N., Weigand, S.D., Murray, M.E., Liesinger, A.M., Petrucelli, L., Senjem, M.L., Knopman, D.S., Boeve, B.F., 2014b. TDP-43 is a key player in the clinical features associated with Alzheimer's disease. Acta Neuropathol. 127, 811–824.

Mackenzie, I.R., Baborie, A., Pickering-Brown, S., Du Plessis, D., Jaros, E., Perry, R.H., Neary, D., Snowden, J.S., Mann, D.M., 2006. Heterogeneity of ubiquitin pathology in frontotemporal lobar degeneration: classification and relation to clinical phenotype. Acta Neuropathol. 112, 539–549.

Mackenzie, I.R., Neumann, M., Baborie, A., Sampathu, D.M., Du Plessis, D., Jaros, E., Perry, R.H., Trojanowski, J.Q., Mann, D.M., Lee, V.M., 2011. A harmonized classification system for FTLD-TDP pathology. Acta Neuropathol. 122, 111–113.

Mackenzie, I.R., Neumann, M., Bigio, E.H., Cairns, N.J., Alafuzoff, I., Kril, J., Kovacs, G. G., Ghetti, B., Halliday, G., Holm, I.E., 2009. Nomenclature for Neuropathologic Subtypes of Frontotemporal Lobar Degeneration: Consensus Recommendations. Springer.

McKeith, I.G., Boeve, B.F., Dickson, D.W., Halliday, G., Taylor, J.-P., Weintraub, D., Aarsland, D., Galvin, J., Attems, J., Ballard, C.G., 2017. Diagnosis and management of dementia with Lewy bodies: Fourth consensus report of the DLB Consortium. Neurology 89, 88–100.

Melamed, Z., Lopez-Erauskin, J., Baughn, M.W., Zhang, O., Drenner, K., Sun, Y., Freyermuth, F., McMahon, M.A., Beccari, M.S., Artates, J.W., Ohkubo, T., Rodriguez, M., Lin, N., Wu, D., Bennett, C.F., Rigo, F., Da Cruz, S., Ravits, J., Lagier-Tourenne, C., Cleveland, D.W., 2019. Premature polyadenylation-mediated loss of stathmin-2 is a hallmark of TDP-43-dependent neurodegeneration. Nat. Neurosci. 22, 180–190.

Mirra, S.S., Heyman, A., McKeel, D., Sumi, S., Crain, B.J., Brownlee, L., Vogel, F., Hughes, J., Van Belle, G., Berg, L., 1991. The Consortium to Establish a Registry for Alzheimer's Disease (CERAD): Part II. Standardization of the neuropathologic assessment of Alzheimer's disease. Neurology 41, 479.

Montine, T.J., Phelps, C.H., Beach, T.G., Bigio, E.H., Cairns, N.J., Dickson, D.W., Duyckaerts, C., Frosch, M.P., Masliah, E., Mirra, S.S., 2012. National Institute on Aging–Alzheimer's Association guidelines for the neuropathologic assessment of Alzheimer's disease: a practical approach. Acta Neuropathol. 123, 1–11.

Murray, M.E., Graff-Radford, N.R., Ross, O.A., Petersen, R.C., Duara, R., Dickson, D.W., 2011. Neuropathologically defined subtypes of Alzheimer's disease with distinct clinical characteristics: a retrospective study. Lancet Neurol. 10, 785–796.

Nag, S., Yu, L., Wilson, R.S., Chen, E.-Y., Bennett, D.A., Schneider, J.A., 2017. TDP-43 pathology and memory impairment in elders without pathologic diagnoses of AD or FTLD. Neurology 88, 653–660.

Nelson, P.T., Dickson, D.W., Trojanowski, J.Q., Jack, C.R., Boyle, P.A., Arfanakis, K., Rademakers, R., Alafuzoff, I., Attems, J., Brayne, C., 2019. Limbic-predominant age-related TDP-43 encephalopathy (LATE): consensus working group report. Brain 142, 1503–1527.

Nelson, P.T., Schmitt, F.A., Lin, Y., Abner, E.L., Jicha, G.A., Patel, E., Thomason, P.C., Neltner, J.H., Smith, C.D., Santacruz, K.S., 2011. Hippocampal sclerosis in advanced age: clinical and pathological features. Brain 134, 1506–1518.

Neumann, M., Sampathu, D.M., Kwong, L.K., Truax, A.C., Micsenyi, M.C., Chou, T.T., Bruce, J., Schuck, T., Grossman, M., Clark, C.M., 2006. Ubiquitinated TDP-43 in frontotemporal lobar degeneration and amyotrophic lateral sclerosis. Science 314, 130–133.

Pankov, A., Binney, R.J., Staffaroni, A.M., Kornak, J., Attygalle, S., Schuff, N., Weiner, M. W., Kramer, J.H., Dickerson, B.C., Miller, B.L., 2016. Data-driven regions of interest for longitudinal change in frontotemporal lobar degeneration. NeuroImage: Clinical 12, 332–340.

Prudencio, M., Humphrey, J., Pickles, S., Brown, A.L., Hill, S.E., Kachergus, J.M., Shi, J., Heckman, M.G., Spiegel, M.R., Cook, C., Song, Y., Yue, M., Daughrity, L.M., Carlomagno, Y., Jansen-West, K., de Castro, C.F., DeTure, M., Koga, S., Wang, Y.C., Sivakumar, P., Bodo, C., Candalija, A., Talbot, K., Selvaraj, B.T., Burr, K., Chandran, S., Newcombe, J., Lashley, T., Hubbard, I., Catalano, D., Kim, D., Propp, N., Fennessey, S., Consortium, N.A., Fagegaltier, D., Phatnani, H., Secrier, M., Fisher, E. M., Oskarsson, B., van Blitterswijk, M., Rademakers, R., Graff-Radford, N.R., Boeve, B.F., Knopman, D.S., Petersen, R.C., Josephs, K.A., Thompson, E.A., Raj, T., Ward, M., Dickson, D.W., Gendron, T.F., Fratta, P., Petrucelli, L., 2020. Truncated

stathmin-2 is a marker of TDP-43 pathology in frontotemporal dementia. J. Clin. Invest. 130, 6080–6092.

Renton, A.E., Majounie, E., Waite, A., Simon-Sanchez, J., Rollinson, S., Gibbs, J.R., Schymick, J.C., Laaksovirta, H., van Swieten, J.C., Myllykangas, L., Kalimo, H., Paetau, A., Abramzon, Y., Remes, A.M., Kaganovich, A., Scholz, S.W., Duckworth, J., Ding, J., Harmer, D.W., Hernandez, D.G., Johnson, J.O., Mok, K., Ryten, M., Trabzuni, D., Guerreiro, R.J., Orrell, R.W., Neal, J., Murray, A., Pearson, J., Jansen, I. E., Sondervan, D., Seelaar, H., Blake, D., Young, K., Halliwell, N., Callister, J.B., Toulson, G., Richardson, A., Gerhard, A., Snowden, J., Mann, D., Neary, D., Nalls, M. A., Peuralinna, T., Jansson, L., Isoviita, V.M., Kaivorinne, A.L., Holtta-Vuori, M., Ikonen, E., Sulkava, R., Benatar, M., Wuu, J., Chio, A., Restagno, G., Borghero, G., Sabatelli, M., Consortium, I., Heckerman, D., Rogaeva, E., Zinman, L., Rothstein, J. D., Sendtner, M., Drepper, C., Eichler, E.E., Alkan, C., Abdullaev, Z., Pack, S.D., Dutra, A., Pak, E., Hardy, J., Singleton, A., Williams, N.M., Heutink, P., Pickering-Brown, S., Morris, H.R., Tienari, P.J., Traynor, B.J., 2011. A hexanucleotide repeat expansion in C9ORF72 is the cause of chromosome 9p21-linked ALS-FTD. Neuron 72, 257–268.

Roberts, R.O., Geda, Y.E., Knopman, D.S., Cha, R.H., Pankratz, V.S., Boeve, B.F., Ivnik, R. J., Tangalos, E.G., Petersen, R.C., Rocca, W.A., 2008. The Mayo Clinic Study of Aging: design and sampling, participation, baseline measures and sample characteristics. Neuroepidemiology 30, 58–69.

Robinson, J.L., Lee, E.B., Xie, S.X., Rennert, L., Suh, E., Bredenberg, C., Caswell, C., Van Deerlin, V.M., Yan, N., Yousef, A., 2018. Neurodegenerative disease concomitant proteinopathies are prevalent, age-related and APOE4-associated. Brain 141, 2181–2193.

Robinson, J.L., Porta, S., Garrett, F.G., Zhang, P., Xie, S.X., Suh, E., Van Deerlin, V.M., Abner, E.L., Jicha, G.A., Barber, J.M., 2020. Limbic-predominant age-related TDP-43 encephalopathy differs from frontotemporal lobar degeneration. Brain 143, 2844–2857.

Rohrer, J.D., Geser, F., Zhou, J., Gennatas, E.D., Sidhu, M., Trojanowski, J.Q., Dearmond, S.J., Miller, B.L., Seeley, W.W., 2010. TDP-43 subtypes are associated with distinct atrophy patterns in frontotemporal dementia. Neurology 75, 2204–2211.

Seo, S.W., Thibodeau, M.-P., Perry, D.C., Hua, A., Sidhu, M., Sible, I., Vargas, J.N.S., Gaus, S.E., Rabinovici, G.D., Rankin, K.D., 2018. Early vs late age at onset frontotemporal dementia and frontotemporal lobar degeneration. Neurology 90, e1047–e1056.

Team, R.C., 2019. R: A language and environment for statistical computing (version 3.1. 2). Vienna, Austria. R Foundation for Statistical Computing; 2014.

Tomé, S.O., Vandenberghe, R., Ospitalieri, S., Van Schoor, E., Tousseyn, T., Otto, M., von Arnim, C.A., Thal, D.R., 2020. Distinct molecular patterns of TDP-43 pathology in Alzheimer's disease: relationship with clinical phenotypes. Acta Neuropathol. Commun. 8, 1–22.

Whitwell, J.L., Boeve, B.F., Weigand, S.D., Senjem, M.L., Gunter, J.L., Baker, M.C., DeJesus-Hernandez, M., Knopman, D.S., Wszolek, Z.K., Petersen, R.C., Rademakers, R., Jack Jr., C.R., Josephs, K.A., 2015. Brain atrophy over time in genetic and sporadic frontotemporal dementia: a study of 198 serial magnetic resonance images. Eur. J. Neurol. 22, 745–752.

Whitwell, J.L., Dickson, D.W., Murray, M.E., Weigand, S.D., Tosakulwong, N., Senjem, M.L., Knopman, D.S., Boeve, B.F., Parisi, J.E., Petersen, R.C., 2012a. Neuroimaging correlates of pathologically defined subtypes of Alzheimer's disease: a case-control study. Lancet Neurol. 11, 868–877.

Whitwell, J.L., Jack Jr., C.R., Parisi, J.E., Senjem, M.L., Knopman, D.S., Boeve, B.F., Rademakers, R., Baker, M., Petersen, R.C., Dickson, D.W., Josephs, K.A., 2010. Does TDP-43 type confer a distinct pattern of atrophy in frontotemporal lobar degeneration? Neurology 75, 2212–2220.

Whitwell, J.L., Weigand, S.D., Boeve, B.F., Senjem, M.L., Gunter, J.L., DeJesus-Hernandez, M., Rutherford, N.J., Baker, M., Knopman, D.S., Wszolek, Z.K., Parisi, J. E., Dickson, D.W., Petersen, R.C., Rademakers, R., Jack Jr., C.R., Josephs, K.A., 2012b. Neuroimaging signatures of frontotemporal dementia genetics: C9ORF72, tau, progranulin and sporadics. Brain 135, 794–806.

Zhang, Y.-J., Xu, Y.-F., Cook, C., Gendron, T.F., Roettges, P., Link, C.D., Lin, W.-L., Tong, J., Castanedes-Casey, M., Ash, P., 2009. Aberrant cleavage of TDP-43 enhances aggregation and cellular toxicity. Proc. Natl. Acad. Sci. 106, 7607–7612.